Chapter 6

COMPARISON BETWEEN OBSERVATION AND THEORY

6.1 An unexpected phenomenon noticed in the observations

As shown in figure (**3.4)** the fiber optic plate in the focal plane of the telescope contained a single fiber in the center of the frame. During the observations this fiber was positioned at the center of the lunar shadow. The purpose of this fiber was to measure the background signal and was to be subtracted from the signals measured by the other fibers that were exposed to the coronal light.

However the shape of the signal measured by the fiber located in the center of the lunar shadow only provided a clue that the observations were affected by scattering. Figure (**6.1**) shows the signal recorded by the fiber at the center of the lunar shadow. This prominently shows the peaks of the Calcium H and K lines. The counts recorded by this fiber are not negligible compared to the counts recorded by fibers exposed to the coronal light. This indicates that we have a problem with scattering light. The extent of scattering could not be envisaged in advance for the simple reason that the true observational condition could not be replicated in the laboratory. However Cram (1976)

pointed out that the bright sources of scattered light at the time of a solar eclipse are prominences and the chromosphere, and these have a spectrum quite unlike that of either the F or K corona. The only remedial measure that was taken in order to minimize scattering was to maintain clean optical surfaces of the optical components in MACS. Although the extent of scattering in the different wavelength regions is very difficult to quantify, nevertheless, it is a hard lesson to be learnt for any future observations. In this regard some of the remedial measures for any future observations are highlighted in section (**6.3**).

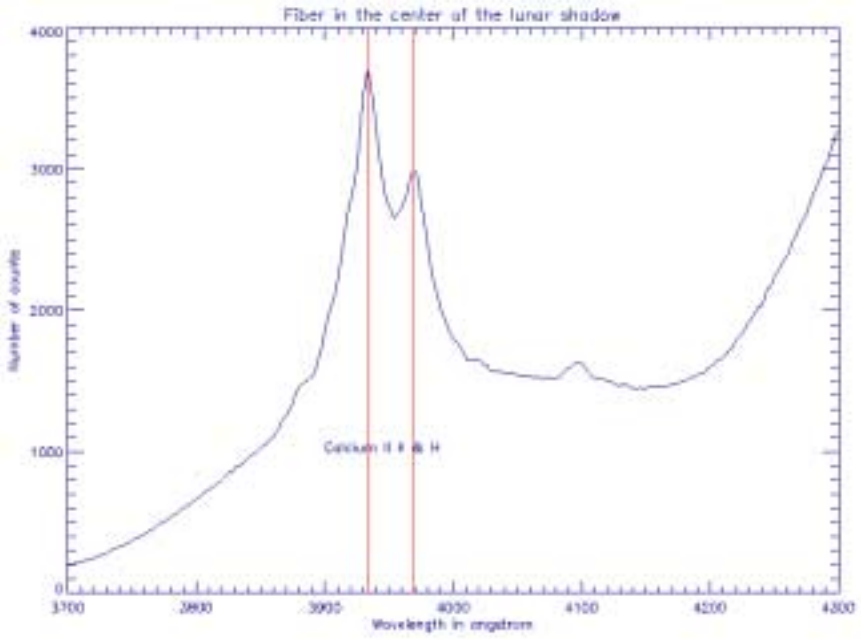

Figure (6.1). The spectrum recorded by the fiber located in the center of the lunar shadow during the eclipse. The x-coordinate corresponds to wavelength scale. The two prominent peaks are associated with the Calcium K & H lines corresponding to 3933.7 and 3968.5 angstroms, respectively.

6.2 Comparison between theory and observation

In chapter-**2** temperature and wind sensitive intensity ratios were identified at particular wavelengths. These intensity ratios were at wavelength positions 4100.0/3850.0 and 4233.0/3987.0, respectively, for temperature and wind measurements. In chapter-**2,** we also showed how to determine the temperature and the wind velocity using the above intensity ratios calculated from the K-coronal intensity spectrum. In contrast to our ratio technique, Ichimoto et al. (1996) chose to determine the coronal temperature by fitting theoretical isothermal K-coronal models to the observed K-coronal spectrum, as shown in figure (**6.2**).

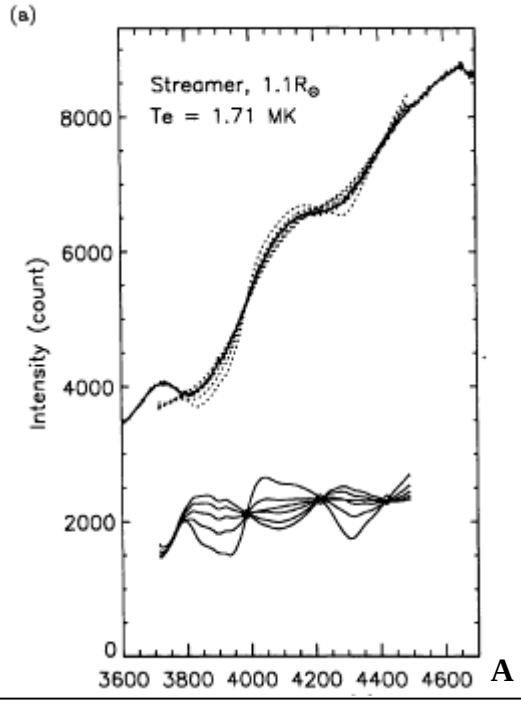

Figure (6.2). Theoretical isothermal K-coronal models fitted to the observed K-coronal intensity spectrum to determine the temperature by Ichimoto et al. (1996). The lower curves show the differences between the observational spectrum and the theoretical models. The model that showed the least difference determined the temperature.

The same temperature measurement, as shown in figure (**6.2**), could also be determined from the measurement of the temperature sensitive intensity ratio. Such ratio calculations were performed using filters centered at the temperature sensitive wavelength positions by J.M. Pasachoff and his team from Williams College, Massachusetts during the total solar eclipse of 11 August 1999 in Romania. N.L. Reginald and J.M. Davila performed the theoretical calculations for predictions of the temperature for the intensity ratios for J.M. Pasachoff and his team. No results have yet been published by Pasachoff et al.

In chapter-**4** the intensity ratio technique was employed to determine the temperature and the wind velocity for several fiber locations. The wind measurements were considered a total failure in this very first attempt to simultaneously and globally determine both temperature and wind velocity at twenty different locations on the solar corona. The reason for this is that the wind measurement is very sensitive to the intensity at 4233.0 angstrom, which is at the high end of the wavelength measurement by MACS. As revealed in figure (**6.1**) the instrumental scattering was high at the high end of the wavelength region thus predicting very high values for the wind velocity measurements. As for the temperature it too suffered from the instrumental scattering. The reason for this is that the temperature is sensitive to the intensity measurement at 3850.0 angstrom and 4100.0 angstrom. As revealed in figure (**6.1**) the strong Calcium Hand K lines in the region of 3900-4000 angstrom seem to have contributed strongly to instrumental scattering. Predicting the contribution due to scattering on the coronal intensity measured

by individual fibers is further compounded by its dependency on wavelength. At this juncture the knowledge of instrumental scattering only provides awareness of the problem of instrumental scattering and remedial measures that need to be considered before any future observations. The sole handicap in such observations is the inability to replicate the experiment in the laboratory in the absence of a coronagraph.

Figure (**6.3**) shows the comparison between experimentally obtained K-coronal spectrum for fiber # 04 with theoretical models for various isothermal temperatures. From the intensity ratio method the wind velocity and the temperature deduced for fiber # 04 are 300.0 km/sec and 1.29 MK, respectively. The theoretical K-coronal models plotted in figure (**6.3**) correspond to a wind velocity of 300.0 km/sec and isothermal coronal temperatures of 0.5MK, 1.0 MK, 1.5 MK and 2.0 MK. In such a scenario the experimentally obtained K-coronal spectrum may be expected to lie between the theoretical models for 1.0 MK and 1.5 MK. However it is obvious that the experimental K-coronal spectrum deviates from the predictions. This deviation can be divided into four distinct regions on the wavelength scale.

1. 3800 – below: In this region the experimental curve falls below the predictions.

2. 3800 – 4000: In this region the experimental curve rises above the predictions.

3. 4000 – 4200: In this region the experimental curve falls below the predictions.

4. 4200 – above: In this region the experimental curve rises above the predictions.

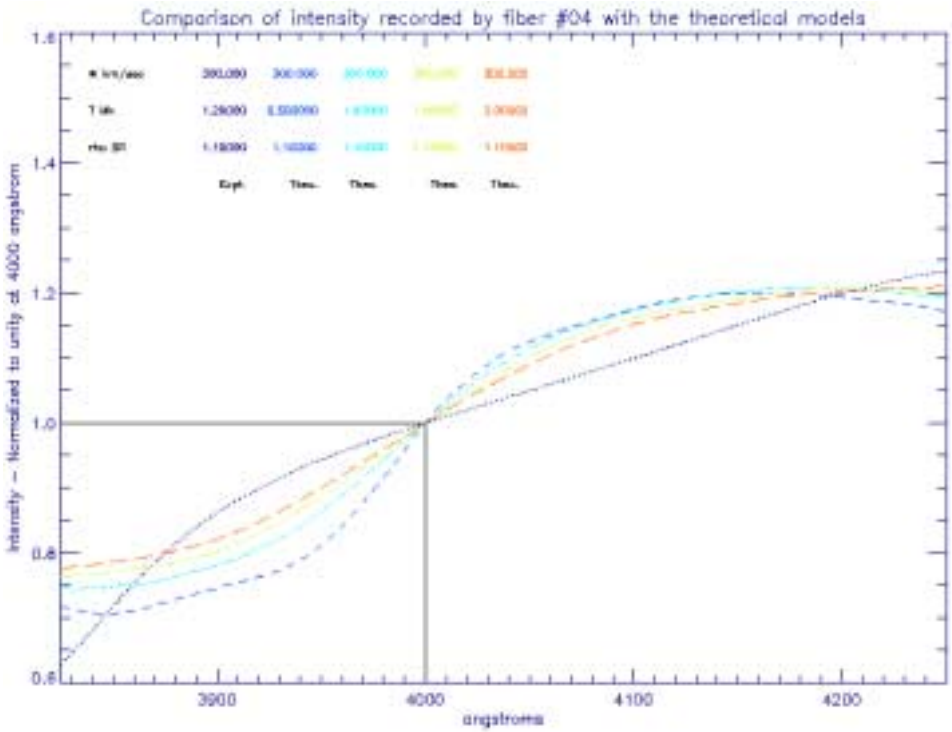

Figure (6.3). This plot shows the comparison between experimentally obtained K-coronal spectrum for fiber # 04 with theoretical models for various isothermal temperatures. From the intensity ratio method the wind velocity and the temperature deduced for fiber # 04 are, 300.0 km/sec and 1.29 MK, respectively. The theoretical K-coronal models plotted in figure (6.3) correspond to a wind velocity of 300.0 km/sec and isothermal coronal temperatures of 0.5MK, 1.0 MK, 1.5 MK and 2.0 MK. In such a scenario the experimentally obtained K-coronal spectrum may be expected to take a position between the theoretical models for 1.0 MK and 1.5 MK. (Expt: = Experimental, Theo: Theoretical)

The comparison between observation and theory for the K-coronal spectrum recorded by fiber # 04, as shown in figure (**6.3**), needs to be considered in conjunction with the extent of instrumental scattering that is depicted in figure (**6.1**). Figure (**6.1**) too can be divided into four distinct regions. Assuming that the signal expected of this fiber located in the center of the lunar shadow to produce a straight line with a positive gradient

signaling a higher background count at higher wavelengths. Based on this assertion, and assuming the signal recorded in the 4000 – 4200 angstrom to represent the correct true background signal, figure (**6.2**) can be divided into four distinct regions.

1. 3800 – below: Some optical component in MACS seems to possess a very low sensitivity to the blue region of the spectrum.
2. 3800 – 4000: The Calcium II K & H lines contribute a large signal in this region.
3. 4000 – 4200: Assumed to represent the true background count.
4. 4200 - above: Scattering is again significant in the high end of the spectrum.

The above properties pertaining to the four distinct regions in the scattered spectrum is similar to the pattern of deviation of the observed K-coronal spectrum of fiber # 04 from the theoretical models, as shown in figure (**6.3**). That is, the very low blue sensitivity in the wavelength region 3800 - below and the higher counts from the scattering of the Calcium II K & H lines in the region 3800 – 4000 angstrom may have caused the observed K-coronal spectrum to dip and rise, respectively, in these regions. The scattering associated with the high end of the wavelength region, i.e. 4200 - above, may have caused the observed K-coronal spectrum to again rise above the predicted level. Figure (**6.4**) is a plot of the superposition of figure (**6.1**) and figure (**6.3**). This shows that there is a certain amount of similarity between, on the one hand, the shape of the scattered spectrum, and on the other hand, the deviation between the predicted and observed K-coronal spectra. In figure (**6.4**), all spectra are normalized to unity at 4000.0

angstrom. It is reasonable to infer from figure (**6.4**) that some proportion of the scattered light spectrum recorded by the fiber located in the center of the lunar shadow has contaminated spectrum recorded by fiber #04. This could explain the deviations between the observed spectrum and the predictions.

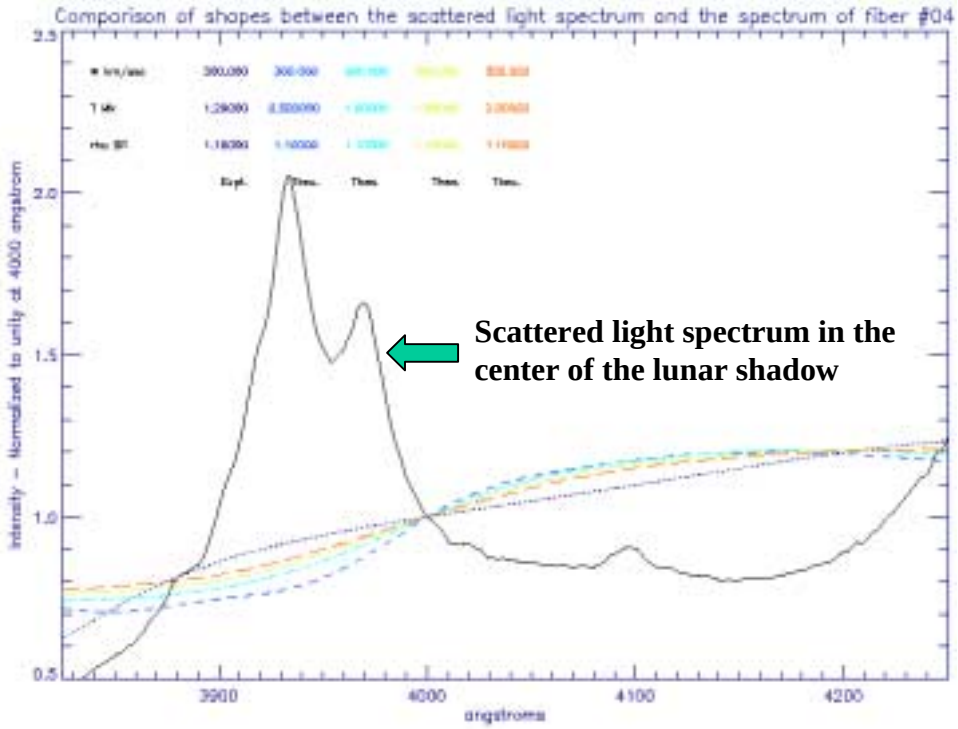

Figure (6.4). A plot of the superposition of figure (6.1) and figure (6.3). The shape of the spectrum recorded by the fiber located in the center of the lunar shadow corresponds with the shape of the observed K-coronal spectrum by fiber #04. The expected location of the observed spectrum is between the theoretical isothermal K-coronal spectra for 1.0 MK and 1.5 MK.

Figure (**6.5**) shows the superposition of the observed K-coronal spectrum for fiber #04 and the theoretical K-coronal spectrum for a wind velocity and isothermal temperature of 300.0 km/sec and 1.29 MK, respectively, and the difference between the two. The wind velocity and isothermal temperature of 300.0 km/sec and 1.29 MK,

respectively, for fiber #04 were determined from the intensity ratio method. From figure (**6.5**) it is apparent that the deviations between the observational and the theoretical spectra are larger at wavelengths of 3900 – 3950 angstroms (where the scattered light spectrum peaks), and are smaller at wavelengths around 4100 angstrom In this regard, the deviations between observed and predicted spectra exhibit certain gross similarities to the shape of the scattered light spectrum. Even a small percentage of the scattered light spectrum being contaminated with fiber #04 could have caused its spectrum to deviate from the theoretical prediction.

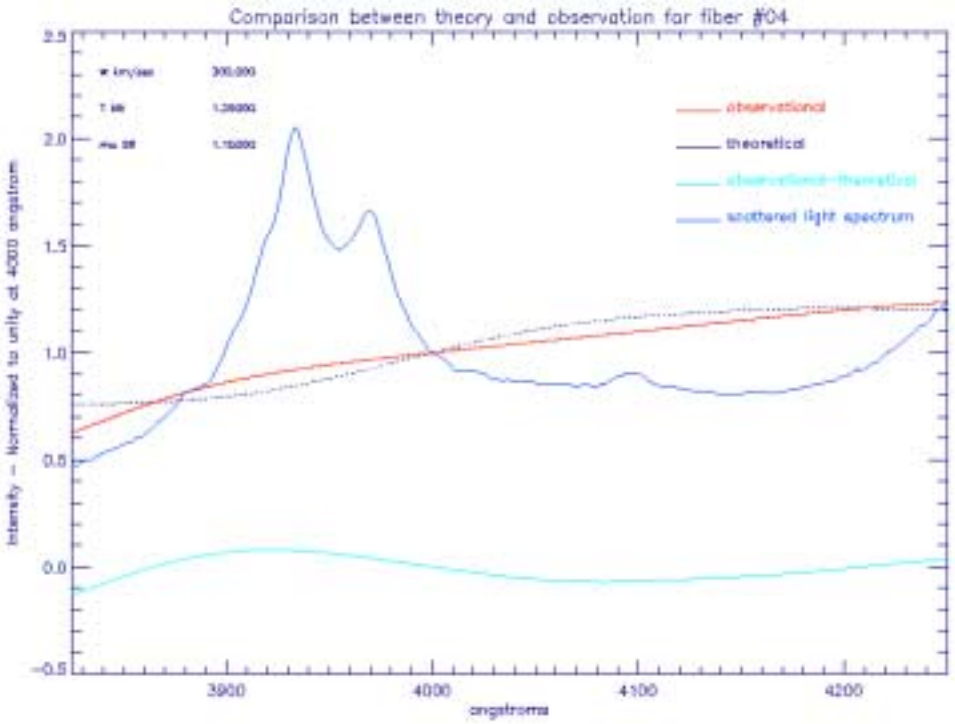

Figure (6.5). A plot showing the observed K-coronal spectrum for fiber #04 along with the theoretical K-coronal spectrum for the wind velocity and temperature derived from fiber #04. The plot also includes the difference between the observational and the theoretical plots along with the scattered light spectrum observed by the fiber in the center of the lunar shadow.

In figure (**6.5**) the areas under the observational and the theoretical spectra are 0.22168834 and 0.22163162, respectively. That is, the difference between the areas is almost negligible. Nevertheless, since the brightest sources of scattered light (chromospheric or prominence material) have spectra which are quite different from those of F- or K-corona, we can now see that even a slight contamination of our coronal data by such scattered light can have a serious effect on the quantitative interpretation of our results. This was pointed out by Cram (1976) who suggested that any observations should avoid such bright sources. However in MACS twenty fibers were exposed to all around the sun and at different heights above the solar limb. As a result, it is almost inevitable that some of our fibers were unfortunately exposed to bright prominence material. The effects due to exposure to these bright sources could be avoided only through a scatter free instrument. In this regard every effort was made to keep instrumental scattering to a minimum. The present experiment, the very first of its kind, reveals the extent and effects of instrumental scattering and the need for more remedial measures in this regard. The same is true of other fibers that were exposed to the coronal light: each was contaminated by scattered light to a greater or lesser extent.

Table (**6.1**) gives the wind and the temperature sensitive intensity ratios for fiber #04 from figure (**6.5**). From table (**6.1**) it is apparent that the wind and temperature sensitive intensity ratios are well matched in spite of the fact that the observational spectrum deviates from the prediction. This may be somewhat fortuitous, since if the amount of scattered light had been different, the observed spectrum might have matched a totally

different theoretical spectrum. This matter is further compounded by the non-existence of any mechanisms to quantify the degree of contamination of instrumental stray light on the individual fiber. In this regard it appears that in spite of the problems caused by the instrumental scattering the temperatures ratios were somehow maintained. Thus the accuracy of the temperature is to within the error estimates made in chapter- (**4 .7)**. That is to within ~**± 6 %** (± 1.2 MK). As for the wind measurements, as discussed in chapter- (**4.7**), its measurement was deemed to have been a failure in the current experimental effort. However the high wind values are in line with the uncertainty of **± 200 km/sec** for a measurement uncertainty of **± 1 %**.

Table (6.1). Comparison of the wind and the temperature sensitive intensity ratios between the observational and the theoretical K-coronal spectrum, for fiber #04. These values are based on figure (6.5).

Fiber #04	**Temp: I(4100)/I(3850)**	**Wind: I(4233)/I(3987)**
Observational	1.531	1.242
Theoretical	1.529	1.242

Figure (**6.6**) shows plots of the observed K-coronal spectrum of fiber #04, as shown in figure (**6.5**), corrected for the scattered light in a crude manner. Here various fractions of the scattered light recorded by the fiber located in the center of the lunar shadow were subtracted from the spectrum recorded by fiber #04. It is evident from figure (**6.6**) that the observed K-coronal spectrum then begins to follow closely the shape of the theoretical K-coronal spectrum implying the influence of the scattered light.

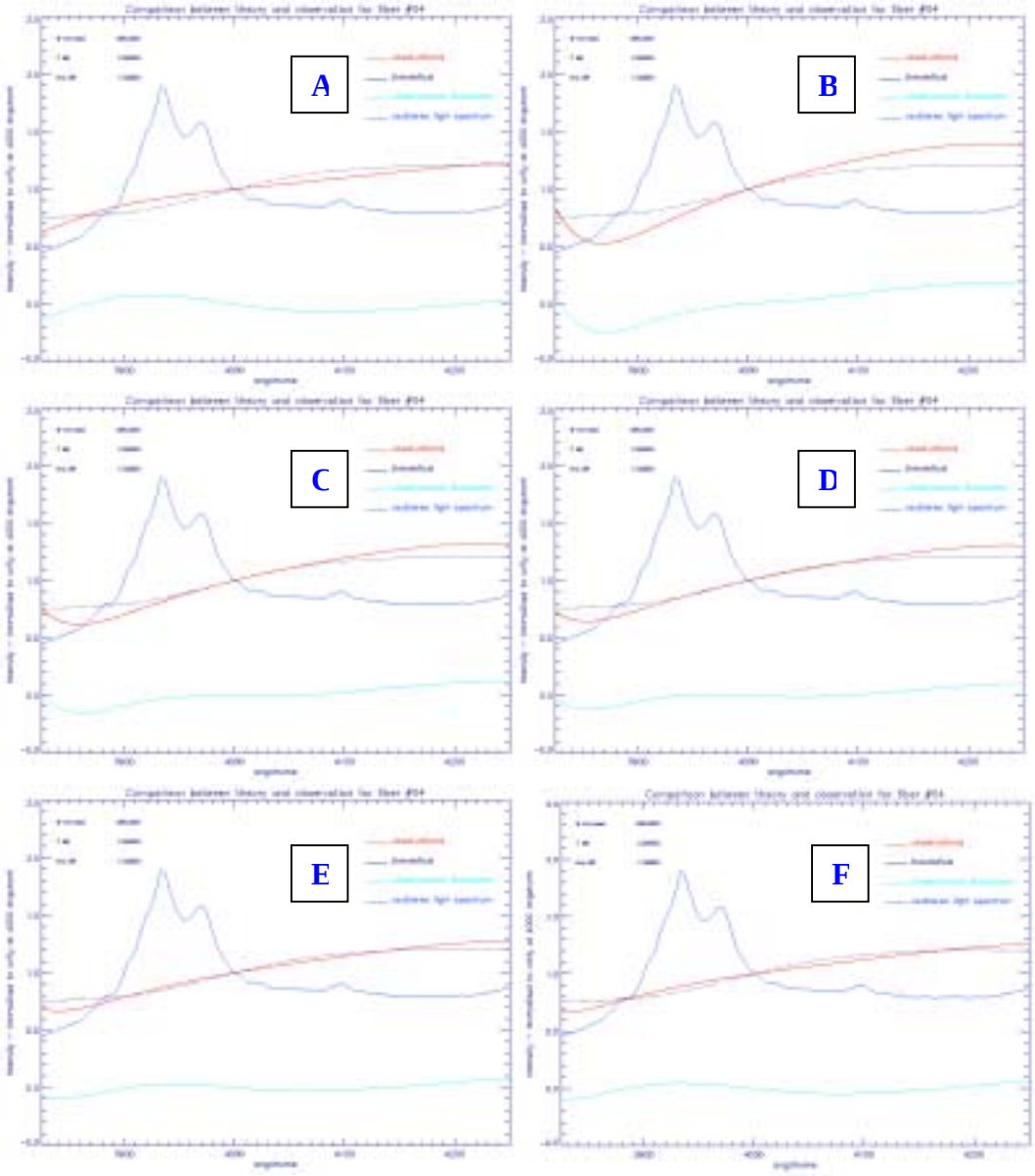

Figure (6.6). Plots showing the effect on the shape of the observed K-coronal spectrum of fiber # 04, as shown in figure (6.5), in comparison with the shape of the theoretical K-coronal spectrum by subtracting various fractions of the scattered spectrum from the observed K-coronal spectrum. A, B, C, D, E and F correspond to a subtraction of 0.0%, 15.0%, 10.0%, 8.0 %, 5.0% and 3.0%, respectively, of the scattered light spectrum recorded by the fiber that was located in the center of the lunar shadow from the spectrum recorded by fiber #04. These plots show that the observed spectrum closely follows the shape of the theoretical spectrum with various fractional subtraction of the scattered spectrum.

A similar pattern as above follows for all the other fibers for which temperatures were determined in chapter- **4**. Instrumental scattering can be minimized only by paying careful attention to the optical quality of the components of the instrument. The stricter the demands on optical quality, the higher the cost will be. The very first operation of MACS in conjunction with the total solar eclipse of 11 August 1999 has shed much light and understanding on the effects of instrumental scattering associated with such observations. Apart from better optics, other remedial measures envisaged for future operation of MACS are listed in section (**6.3**).

6.3 Remedial measures

The principle and the method described in this thesis is unique in its character that allows for the simultaneous and global measurements of the thermal electron temperatures and the solar wind velocities on the solar corona using the shape of the K-coronal spectrum. However the steps described in section (**4.6**) in isolating the K-coronal spectrum from a terrestrial observation in conjunction with an eclipse are beset with problems. The main problems that arise from terrestrial observation during an eclipse are time constraints and state of the sky. Apart from these, there are other difficulties that arise in connection with the data analysis. We summarize these here.

1. In order to determine the wavelength sensitivity of our instrument, we have assumed that the sky spectrum recorded by MACS (corrected for Rayleigh scattering) should match the photospheric spectrum depicted in figure (**2.1**). The comparison between the two spectra shown in figure (**4.21**) demonstrates clearly the nature of the

difficulties we face in this regard, especially close to the Ca line at 3933.7 angstrom and regions at 4000.0 angstrom. Since this method depends on the shape of the K-coronal spectrum these inadequacies, although seem to be irrelevant, do affect the shape of the K-coronal spectrum in a significant manner. However a near perfect wavelength sensitivity curve could be obtained with the use of absolute wavelength calibration using sources of known strengths as commonly done for all advanced instruments with optical elements. This suggests that in this particular experiment the derivation of the wavelength sensitivity curve for MACS was limited in its accuracy by choice.

2. Another problem arises from our assumption that the F-corona must be allowed for in our Rayleigh-corrected MACS sky spectrum. The intensity of the F-corona (which depends on the properties of interplanetary dust between the sun and the earth) has some wavelength dependence, perhaps proportional to $\sqrt{\lambda}$. However on the assumption that the F-corona is unpolarized while the K-corona is polarized (although only orthogonal scattering gives complete polarization as per equations (**A.48**) and (**A.49**) there exists an easy practical means to determine the contribution from F-corona. This is done by observing the corona through a polarized filter with the polarization axis at minimum of three known angular positions. A detailed explanation could be found in Golub and Pasachoff (1997). The only concern that hinders this easy maneuver in conjunction with an eclipse is the time constraints. This suggests that the ideal platform to use MACS be in tandem with a coronagraph.

3. The instrumental stray light could be reduced to a great extent only through superior optics. A fair estimate of the distribution of the instrumental stray light could also be estimated by placing many more fibers in the shadow of the moon and outside the field of view in the focal plane of the telescope as depicted in figure (**6.7**).

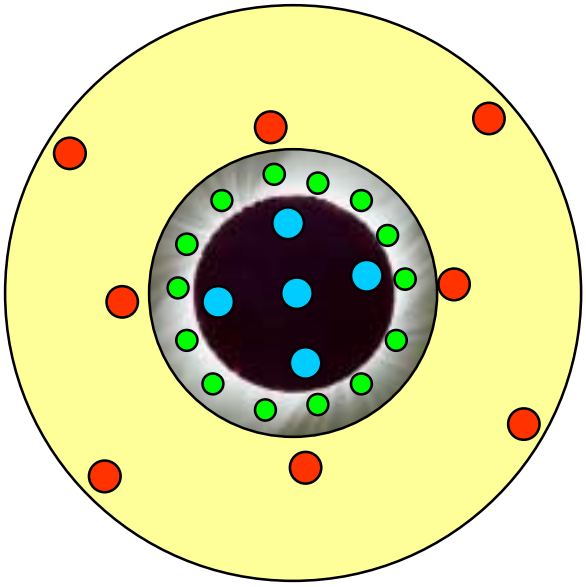

Figure (6.7). The extra fibers placed in the shadow of the moon and outside the field of view in order to record the instrumental stray light distribution.

4. Another important deficiency in MACS in its present state is in its inability to simultaneously visually image the focal plane during the observations. This prevented us from knowing whether the fibers stayed in focus at their intended locations. Deviations from the intended positions can arise from slight movements of the telescope due to wind, and also due to deficiencies in the tracking mechanism. This understanding could be easily satisfied by attaching a CCD-based video camera to the viewfinder of the telescope that in turn is co-aligned with the telescope. The live

video image of the sun through a sun filter projected on a TV screen, at least from one hour prior to the first contact, can be placed on a suitable 2_D grid and its course followed for tracking purposes. The bright pixels prior to the first contact should appear as dark between the second and the third contacts with the sun filter removed. In order to achieve this goal, the viewfinder and the telescope should be perfectly aligned. Although this enables us to monitor the tracking efficiency it does not prove the centering of the sun on the image plane of the telescope. To accomplish this the following maneuver could be followed.

(a). First center the sun's image through the sun filter on a reticle eyepiece. The reticle pattern in the Meade brand is a double cross line with two concentric circles. At this stage if the viewfinder is perfectly aligned with the telescope then the sun's image seen through a video recorder attached to the viewfinder should display the sun's image at the center of the detector. Centering on the reticle eyepiece and making adjustments to the telescope's orientations can be carried out alternatively until the image remains centered on the viewfinder and should satisfy the tracking efficiency.

(b). Then attach a camera with the lenses demounted for prime focus photography of the sun through a sun filter at the focal plane of the telescope. For the Meade brand of 12-inch Schmidt_Cassegrain telescopes one end of the #62-T adapter connects to the F/6.3 focal reducer and the other end threads into a universal T-adapter with bayonet-mount unique to the brand of 35mm camera and focus the image. This should facilitate the focusing for the experiment since the fiber optic plate too will be located

at the prime focus of the telescope during observations. If step (**a**) was successfully performed then the image should be centered too.

However the above features do not yet allow for the simultaneous imaging of the coronal image formed on the front surface of the fiber optic plate. The following optical feature as shown in figure (**6.8**) may be contemplated for MACS in order to obtain simultaneous imaging of the image formed on the focal plane. In figure (**6.8**) the fibers are embedded on an optical flat (well polished reflecting surface facing the telescope) along with a very thin high transmission glass surface (AB) inclined at 45^0 to the optical axis and with a semi-reflecting coating on the side facing the fiber optic plate. The reflected image from (AB) is a copy of the image formed on the fiber optic plate with dark dots marking the light transmitted through the fibers. Such an image will identify the actual location observed by each of the individual fibers on the corona. This is ideal to be used in attachment to a coronagarph. This is because any additional photons lost in the transmission through the additional optical component could be compensated by a longer integration time.

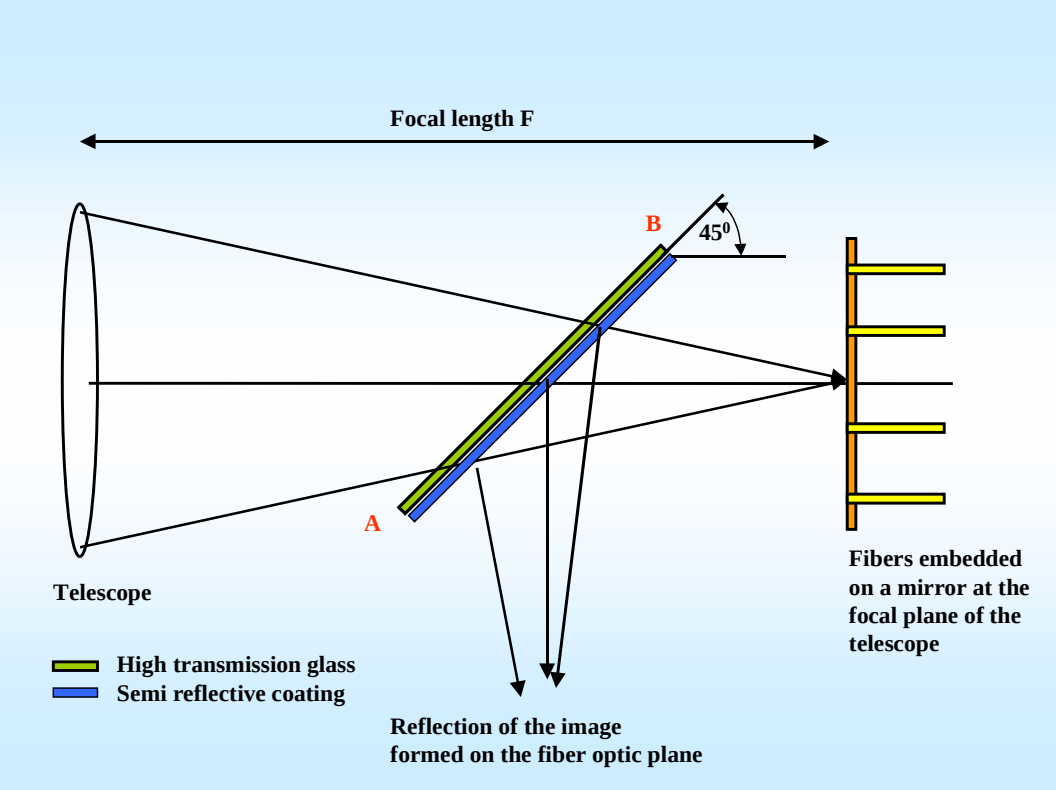

Figure (6.8). A schematic diagram showing the introduction of a very thin high transmission glass surface (AB) inclined at 45^0 to the optical axis with a semi-reflecting coating on the side facing the fiber optic plate along with the fibers embedded on an optical flat. This alteration will enable the simultaneous imaging of the image formed on the fiber optic plate.

The proposal (NRA:99-OSS-01) to build a coronagraph to accommodate MACS at a cost of ~$ 500,000.0 has been approved by the NASA's Office of Space Science. NASA's Goddard Space Flight Center and The Catholic University of America will jointly build this instrument over the next three years. Possibilities for observing sites include Sacramento Peak, Hawaii and the Canaries.